LUPINE PUBLISHERS

Modern Approaches on Material Science

DOI: 10.32474/MAMS.2021.04.000200

ISSN: 2641-6921

Review Article

Metal Chemosensors, Its Classification and Application

Hayat Ullah*[1], Fazal Rahim[2], Fahad Khan[2], Imad Uddin[3], Misbah Ullah Khan[4], Shaheed Ullah[1], Zarif Gul[1], Munzer Ullah[5]

[1]*Department of Chemistry, University of Okara, Okara-56300, Punjab, Pakistan*

[2]*Department of Chemistry, Hazara University, Mansehra-21300, Khyber Pakhtunkhwa, Pakistan.*

[3]*Department of Chemistry, University of Haripur, Haripur-22620, Khyber Pakhtunkhwa, Pakistan*

[4]*Center for Nano-Science, University of Okara, Okara-56300, Punjab, Pakistan*

[5]*Department of Biochemistry, University of Okara, Okara-56300, Punjab, Pakistan*

***Corresponding author:** Hayat Ullah, Department of Chemistry, University of Okara, Okara-56300, Punjab, Pakistan

Received: November 8, 2021 **Published:** November 22, 2021

Abstract

Sensors play an important role in detection of various cation, anions and neutral molecules in chemical and biological samples and have found much interest in the three decades. The sensors bind with analyte species, which lead to change in electron density on sensor molecules and cause changes in its signals or color. Varieties of chemical sensors are used including cationic and anionic and neutral molecules sensors. Molecular recognition and molecular transduction take place in chemical sensing. Generally, a chemosensors consist of three parts, receptor which is binding site, unit whose properties change with binding and spacer.

Keywords: Chemosensors; Application of chemosensors; Classification of chemosensors

Introduction

A Chemosensors is a substance capable of changing color or signal in absorption or emission spectra in the presence of certain specific species with definite concentration which indicate its presence or absence. The information is obtained in the form of a measurable physical signal that is linked with the certain chemical species concentration called analyte [1]. The chemosensors may be broadly classified into two categories.

1. Cation's sensors
2. Anion's sensors

Cation Sensors

Optical cation sensing was initially started for metal ions not having its own spectra in the visible region, has been broadly studied. With the better understanding of host-guest chemistry of crown ethers, it became easier to develop chromogenic sensors for metal ions. Later many outstanding examples of chromophoric and fluorophoric receptors for different cations have been prepared and studied.

I. Chromogenic cation sensors: The chromogenic cation sensors may be grouped into three broad categories [2].

a. Chemosensors for photometry in organic media: These chemosensors mostly function in organic media only. This class includes neutral and few protonic moiety dependents on their net charge when form complex with metal ions. In neutral chemosensors the net electronic charge transfer from the donor to acceptor end inside chromophore. In these chemosensors both intermolecular and intramolecular electron donor acceptor interactions involve, causing metal induced bathochromic or hypochromic spectral shifts. Thus the metal binding with chemosensor affects the electronic state (ground and excited) of chromophore with respect to the corresponding electronic state of the un-complex chromophore. In protonic chemosensors, various functionality like azophenol, nitro phenol having acidic protons play vital role in the chemosensor skeleton.

b. Chemosensors for extraction photometry: In this class anionic type chemosensors are mostly involve having proton-dissociable group which is a part of the chromophore. These chemosensors interact with metal ions which are shown in the form of optical properties. If the singly charged anion is produced upon deprotonating, then it gives charge-neutralized complex with monovalent metal ion which is from aqueous solution extractable to a water-immiscible organic solvent. Occasionally receptors have two anionic side arms results in divalent metal ions molecules

extraction. The potential of these chemosensors are greatly affected by the steric orientation of the anionic group and hollow of the receptor to put up the specific metal ion.

c. Chemosensors for photometry in aqueous media: These chemosensors are specifically designed in aqueous media for metal photometry, instead of using lethal and volatile organic solvents as well as phase separation step which is required in extraction photometry.

II. Fluorogenic cation sensors: Large number of fluorescent signaling systems manipulating the photo induced intramolecular electron transfer (PET) mechanism for metal ions detection are reported. These sensor are planned in such a way to covalently link fluorophores with electron donating atoms of acyclic or macro cyclic receptors. The binding site in the receptor contributes a lone pair of electron to the excited fluorophore through PET and as result the excited fluorophore comes to the ground state by a non-radiative pathway, trigger quenching of fluorescence. The metal ion takes this lone pair through bonding; the PET is blocked, resulting in the recovery of fluorescence. A system with fluorescent on/off ability can possibly act as a molecular photonic switch, which is the utmost significant component of any true photonic device. Keeping in view the above techniques, some admirable receptors for numerous analytes have been prepared and checked for use in medical diagnostics, physiology and in environmental chemistry. Some chromogenic receptors based on crown ethers [3], podands, calixarenes, thiacalixarenes and azacrown-calixarenes have been also reported [4,5] (Figure 1).

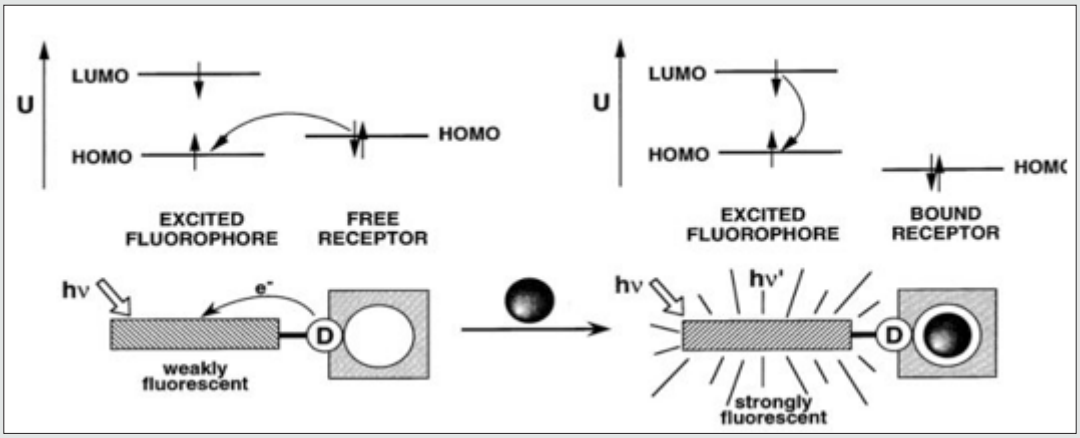

Figure 1: Schematic diagram showing mechanism of ion recognition by fluorescent PET sensors.

Anion Sensors

The chromogenic anion sensors may be generally divided into two main classes, following the classification put forth by both P. A. Gale [6] and Tuntulani et al., [7].

i. Metal and Lewis acid based chromogenic hosts

ii. Nonmetal based chromogenic hosts

(I) Metal and Lewis acid based chromogenic hosts: In metal involved chromogenic hosts, the color change comes from either the color of metals or metal complexes, particularly transition metal ions, whose electronic behavior are altered upon coordination with anions. The anions possibly will also remove the coordinated chromophore to give a colorimetric response. Also, coordination aspects, the color change can came from reactions of chromogenic hosts or indicators and anions. Such chromogenic anion sensor can also be called a "chromoreactant". When a reaction occurs, the conformed host will certainly change its electronic properties, which results in an observable color change. The role of the metal ions in these receptors may be either it acts as non- coordinating moiety but changing its physical properties in the presence of anion, coordination site for the anions or as an electron withdrawing component in a system so as to enable attack of anion on it [8-10]. Several outstanding reviews are also available in the literature on metal ion based anionic sensors [11-15].

(II) Nonmetal based chromogenic hosts: Anion sensors based on nonmetal chromogenic hosts use H-bonding and/or electrostatic interactions for carrying out the job. Limiting here to this group of anion sensors, numerous such systems have been reported like amide [16], pyrrole [17,18], urea and thiourea [19,20], azo dye [21], naphthalene and naphthalimide [22], porphyrin units having neutral hosts [23], ammonium and polyammonium [24], guanidinium, or thiouronium [25] possessing cationic hosts. Several outstanding reviews on fluorogenic/chromogenic are also available in the literature [26], on guanidinium [27], calixarene [28] and urea based receptors. In these neutral or positively charged receptors, the polarized N-H part behaves as H-bond donors to anions. Neutral ligands donate the loan pair of electrons to metal and neutral receptors give H-bonds to the anion. Consequently, metal-ligand complex formation can be studied in any solvent, which make sure solubility of the reactants. This study is preferably performed in aprotic media in order to evade competition for the anion through H-bonding in solvents. The recognition process in these cases normally involves either H-bonding or completes deprotonating of -N-H protons or a stepwise process starting from H-bonding to dissociation of proton [29]. In some cases it involes in

stepwise deprotonation of two protons, without the intermediate step related to the H-bonding. As suggested by Fabbrizzi et al. in this host-guest complexation, subsequently following equilibria may take place in solution, comprising a neutral receptor LH2 and the anion X [30].

$$LH_2 + X^- \rightleftharpoons [LH_2\text{---}X]^-$$

$$[LH_2\text{---}X]^- + X^- \rightleftharpoons [LH]^- + [HX_2]^-$$

$$[LH]^- + 2X^- \rightleftharpoons L^- + [HX_2]^-$$

Here the first step relates to a H-bonded complex and in the second step abstraction of a proton from the complex involves to give a mono deprotonated derivative LH^- which might give further fully deprotonated L according to step-3 at greater concentrations of the anion. The incidence of de-protonation is greatly reliant on the inherent acidity of LH, $[HX2]^-$ stability and the solvent polarity. Still it is an effective and sensitive technique of anion sensing [31]. The variety of nanoparticles has been reported in literature for the sensing of various metal ions. Here in this study we focus only on various type of gold nanoparticles interaction with metal ions.

Glutathione-Protected Fluorescent Gold Nanoclusters

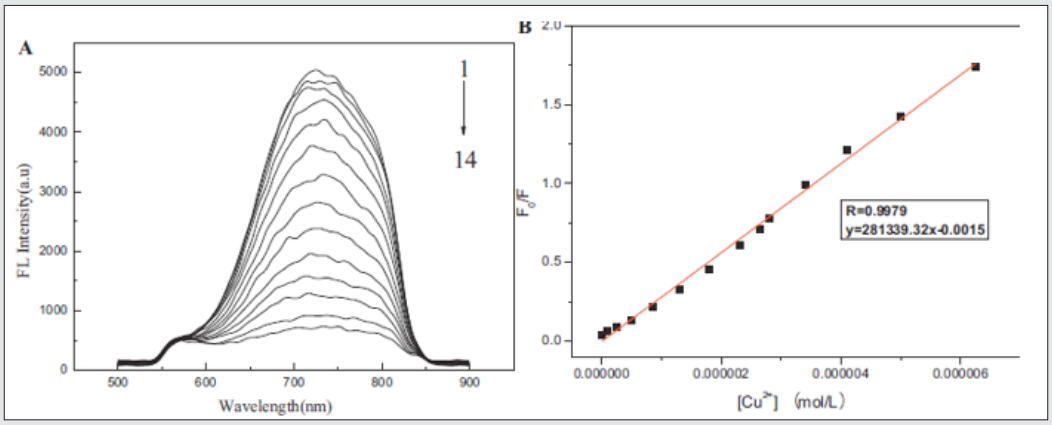

Figure 2: (A) Fluorescence response of 0.05 mg/mL GS-Au NCs upon addition of different concentrations of Cu^{2+} solution. (B) Linear relationship between F0/F and the concentration of Cu^{2+}.

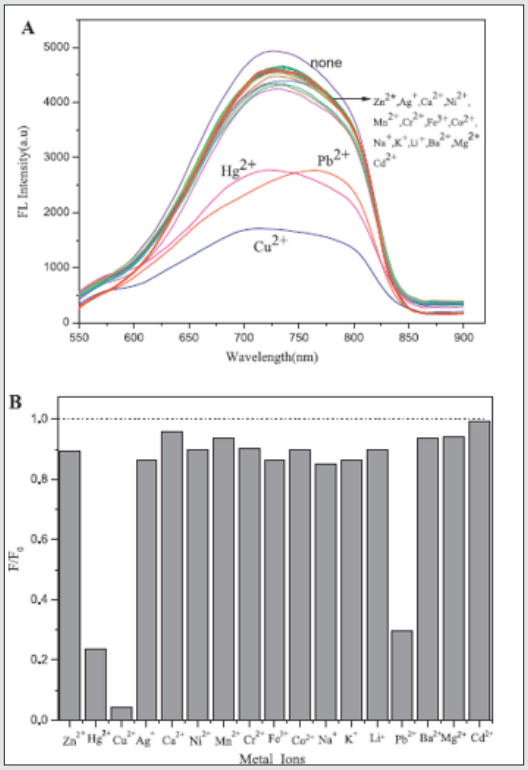

Figure 3: (A) and (B) Effect of different metal ions on the fluorescence of GS-Au NCs in PBS buffer (pH 7.0).

The glutathione (GS)-protected Au nanoclusters (GS-Au NCs) has been reported as a novel fluorescent probe for copper ion (Cu^{2+}) detection. The sensing behavior of GS-Au NCs toward metal ions beed buffered aqueous media. The Cu^{2+}, Hg^{2+} and Pb^{2+} metal ions were establish to quench efficiently the GS-Au NCs fluorescence emission upon studying various metal ions. This nanocluster have the ability to differentiate among these metal ions. The $Cu^{2+}$and Hg^{2+} (or Pb^{2+}), It was observed that in the presence of Pb^{2+}, the GS-Au NCs solution first appeared turbidity, but with ethylene diamine tetraacetate added to the solution, the fluorescence recovered and the turbidity vanished; in the presence of Hg^{2+}, EDTA could not recover the quenched fluorescence of GS-Au CNs by Hg^{2+}, which is in contrast with Pb2+ and Cu2+. The Cu^{2+}limit of detection was approximately 86 nM based on the fluorescence quenching and linear fluorescence response in the Cu^{2+} concentration. The high sensitivity and selectivity toward Cu^{2+} among various metal cations make GS-Au NCs a good candidate for fluorescent sensors of Cu^{2+} + ions [32]. The fluorescence sensing experiments of GS-Au NCs toward Cu^{2+} were also examined for pH effect and pH 7.0 was found to be optimum (Figure 2A). The quenching in the presence of Cu^{2+} can be recognized due to complexation between the GS-ligands of the GS-Au NCs and Cu^{2+} ions (Figure 2B). The fluorescence sensing selectivity for Cu^{2+}, Hg^{2+} and Pb^{2+}, among seventeen kinds of metal ions such as Zn^{2+}, Hg^{2+}, Cu^{2+}, Fe^{3+}, Co^{2+}, Na+, K+, Ag+, Li^{2+}, Pb^{2+}, Ba^{2+}, Ca^{2+}, Mn^{2+}, Cr^{2+}, Ni^{2+}, Mg^{2+} and Cd^{2+} were confirmed by UV and florescence spectrophotometry (Figure 3A,B) Table 1.

Table-1: The coexistence ion effect on the sensing of Cu^{2+}

Coexistence ion	Concentration (mol/L)	(F0 –F) /F (%)	Coexistence ion	Concentration (mol/L)	(F0 –F) /F (%)
Fe^{3+}	5×10^{-5}	0.8	Na^{+}	5×10^{-5}	0.4
Ba^{2+}	5×10^{-5}	1.2	Li^{+}	2.5×10^{-5}	2.0
K^{+}	5×10^{-5}	0.7	Mg^{2+}	5×10^{-5}	0.6
Ag^{+}	5×10^{-5}	3.1	Cr^{2+}	5×10^{-5}	1.5
Co^{2+}	2.5×10^{-5}	1.8	Cd^{2+}	5×10^{-5}	1.6
Zn^{2+}	5×10^{-5}	0.6	Ca^{2+}	5×10^{-5}	– 0.7
Mn^{2+}	5×10^{-5}	0.6	Pb^{2+}	2.5×10^{-5}	2.2
Hg^{2+}	5×10^{-6}	3.2	Ni^{2+}	2.5×10^{-6}	1.6

Gold Nanoparticles having Fluorescent Cysteine-Coumarin Probes

Emissive molecular probes based on amino acid moieties are very attractive due to their use as new building blocks in peptide synthesis [33]. The coumarin probes (1 and 2) were synthesized and fully characterized. Their sensing capacity toward alkaline earth, transition, and post-transition metal and their acid base behavior (H+, OH) were explored by absorption and fluorescence spectroscopy in absolute ethanol. Compound 1 displays a strong complexation constant with the soft metal ions Cd^{2+}, Zn^{2+}, and Ag+. Compound 2 shows a great fluorescence quantum yield, and it might be used as a non pH-dependent fluorescent probe (Figure 4). Gold nanoparticles having compounds 1 and 2 as stabilizers were got by using a reductive method and were characterized by UV-vis, TEM and light scattering. The new stable Cou@AuNPs acted as supramolecular chemosensors, selective for Hg^{2+}, with a simultaneous change of color from pink to dark red/brown [34]. The sensorial ability of both compounds toward Ca^{2+}, Cu^{2+}, Zn^{2+}, Cd^{2+}, Hg^{2+}, Ni^{2+}, Ag+, and Al^{3+}metal ions were examined. Both compounds do not show any photo-physical changes under acidic conditions, but in basic media show an intense emission quenching of fluorescence emission. This is possibly due to the of the amine group deprotonation, which produces a photo-induced electron transfer (PET) process from the lone pair of electrons located in the nitrogen atom to the excited chromophore (Figure 5). The addition of metal ions to compound 1 in absolute ethanol does not change the ground state, but on the contrary, the excited state is quenched by metal ions like Zn^{2+}, Cd^{2+}, Ag+, and Hg^{2+} (Figure 6). Though, in other metals studied, the quenching was smaller. One of the possibilities is that in the ground state the metal ion is interacting with the amino acid unit far from the chromophore, and then altering its position after the irradiation for the carbonyl of the lactone in the excited state, making a quenching in the fluorescence emission [35,36] (Scheme-1).

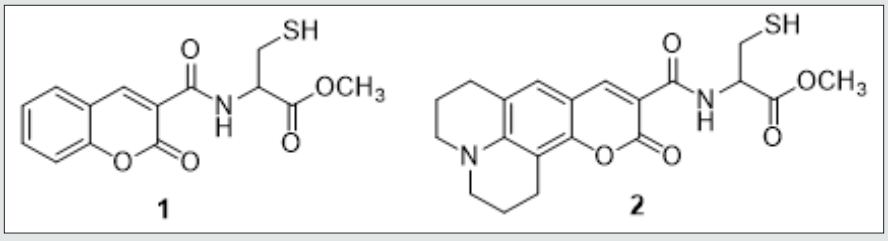

Figure 4: Structure of Compounds 1 and 2.

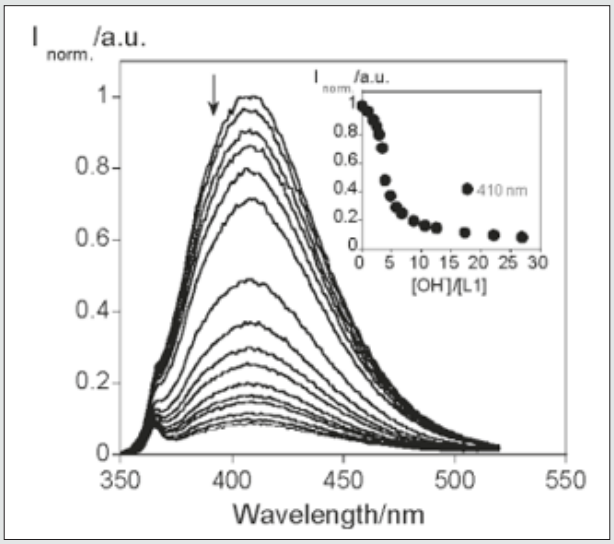

Figure 5: Spectrofluorimetric titration of compound 1 with the addition of OH- in absolute ethanol.

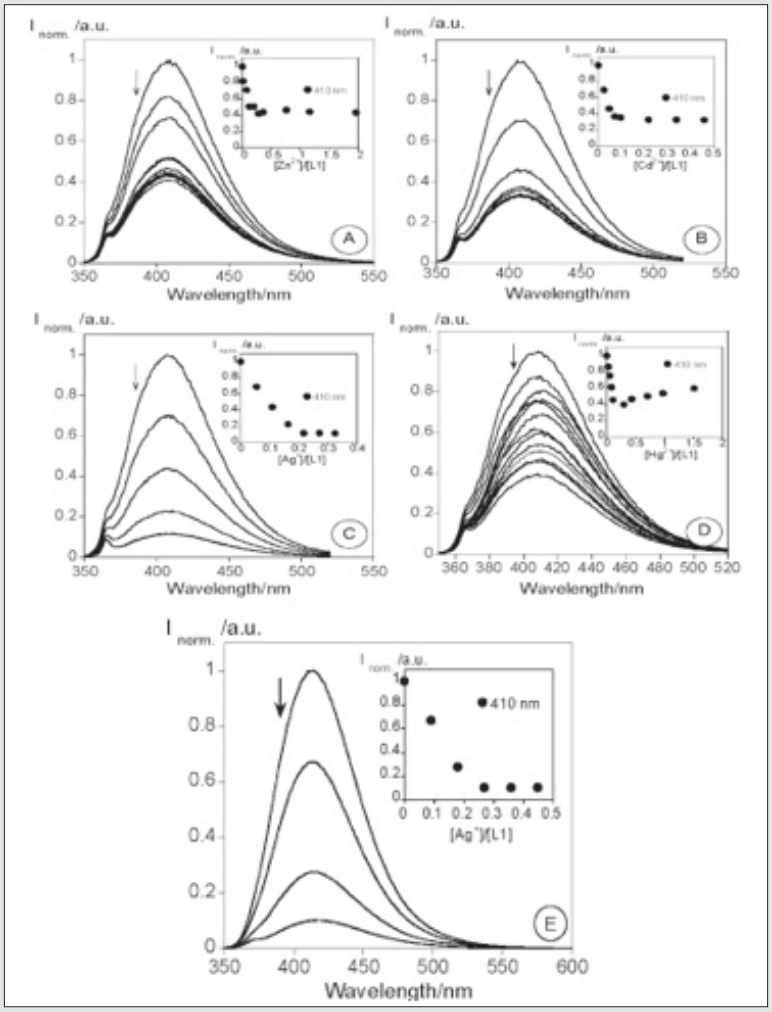

Figure 6: Spectrofluorimetric titration of compound **1** in the presence of Zn^{2+} (A), Cd^{2+} (B), Ag^{+} (C), and Hg^{2+} (D) in absolute ethanol and in the presence of Ag^{+} (E) in a mixture of water/absolute ethanol (80:20).

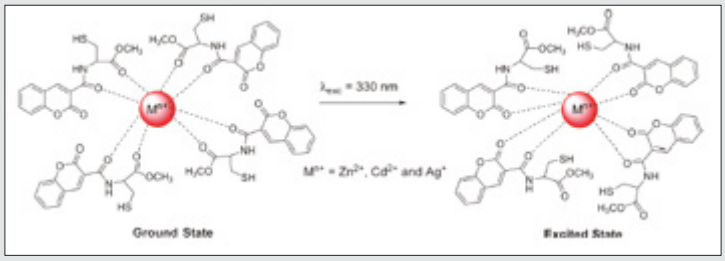

Scheme 1: Coordination Proposed for Zn^{2+}, Cd^{2+}, and Ag^{+} Ions with Compound **1**

The stoichiometry of each metal complex was predicted by the Job's plot in which one metal ion is coordinated by 4 equal of 1. As an example, (Figure 7) shows the absorption and emission of 2 in the presence of Ni^{2+} and Al^{3+}. The addition of Ni^{2+} or Al^{3+} (Figure 7 A, B) produces a decrease in the absorption spectrum with a concomitant appearance of a new shoulder or band. This band appears due to the participation of the carbonyl group in complexation [37]. Comparing both coumarin derivatives, 1 and 2, we can conclude that 1 is more affected by the metal ion complexation than 2. This fact can be observed in the column graph reported in (Figure 8).The AuNPs coated with compounds 1 and 2 were obtained by the Brust methodology on the basis of the reduction with NaBH4 (Scheme 2) [38]. The formation of the nanoparticles can be observed because of the appearance of the gold plasmonic resonance band at 520 nm and because of the change in color from orange to red. These AuNPs were not emissive because the luminescence of the coumarin was totally quenched by the gold metal core. The size of 1 and 2 nanoparticles of ca. 3.3 (1.1 nm and ca. 2.6 (1.2 nm, respectively, was measured by DLS. To explore the potential application of these functionalized small stable gold nanoparticles (AuNPs) as chemosensors for toxic, heavy, and soft metal ions Hg^{2+}, Cd^{2+}, Zn^{2+}, and Ag+, several metal titrations were performed following the modifications in the surface plasmonic resonance band (SPRB) [39]. Only in the case of mercury (II) was an effect observed. The addition of Hg2+ showed a color change from pink to dark red/ brown in both systems (Figure 9), as well as an increase of 100-fold in the nanoparticle size, raising the AuNPs aggregation.

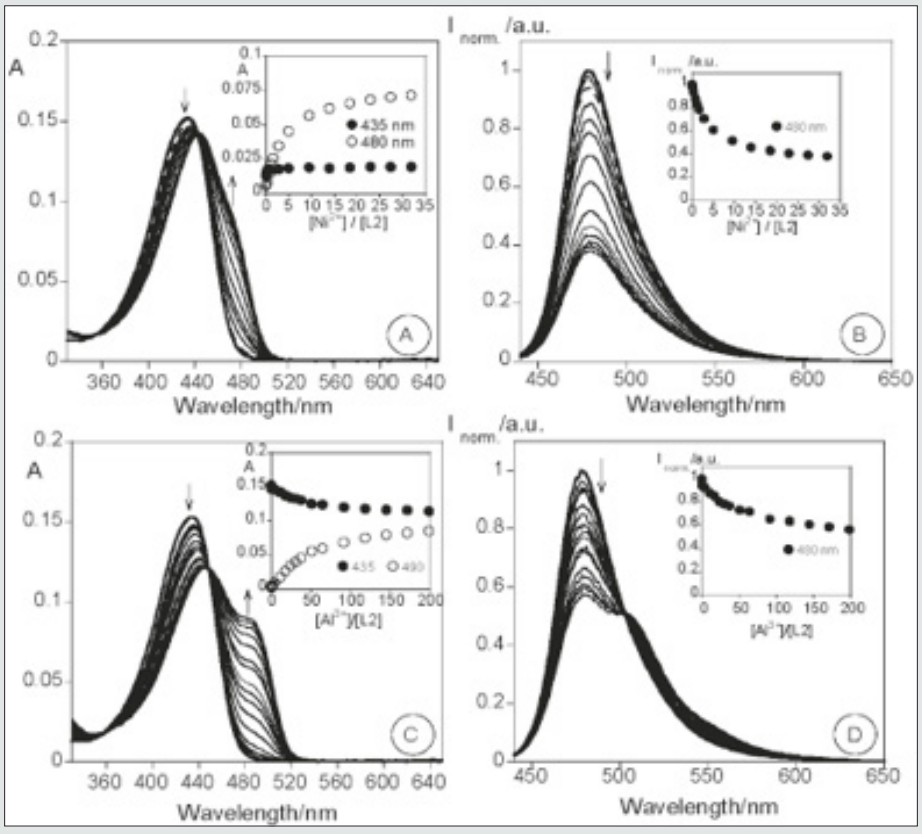

Figure 7: Spectrophotometric and spectrofluorimetric titration of compound 2 in the presence of Ni^{2+} (A), (B); Al^{3+} (C), (D);

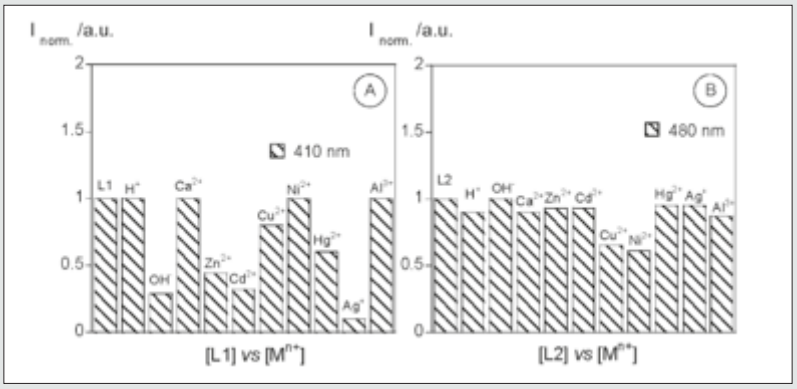

Figure 8: Normalized fluorescence of compounds **1** (A) and **2** (B) in the presence of H^+, OH^-, Ca^{2+}, Zn^{2+}, Cd^{2+}, Cu^{2+}, Ni^{2+}, Hg^{2+}, Ag^+, and Al^{3+} in absolute ethanol.

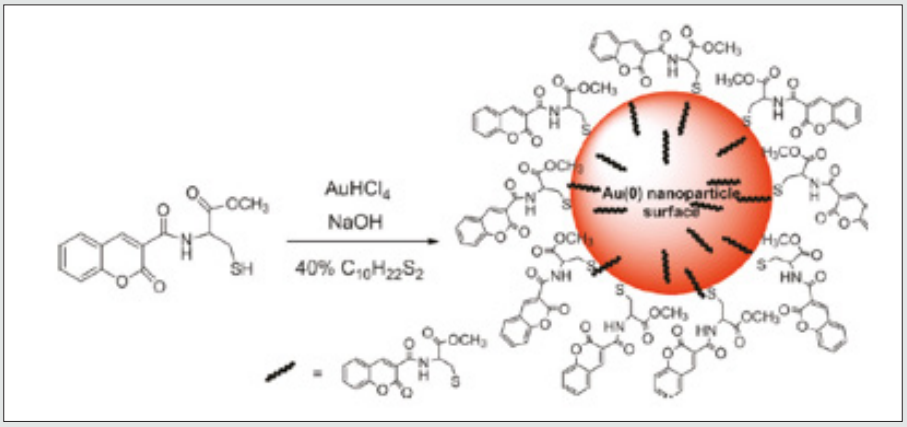

Scheme 2: General Synthetic Pathway for Gold Nanoparticles with 1

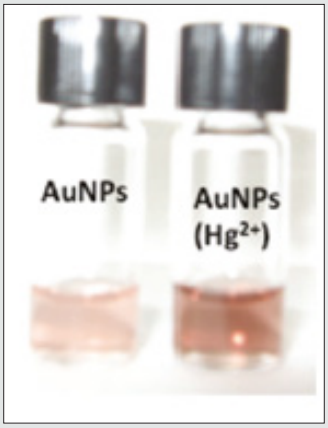

Figure 9: Naked-eye detection of Hg^{2+} by AuNPs **1** and after titration with Hg^{2+} in dichloromethane.

The spectrophotometric titration with Hg^{2+} for AuNPs with compound 1 and 2. On the basis of the Lambert Beer law and the extinction molar coefficient at 330 and 435 nm for free 1 and 2, respectively, it was possible to determine the approximate concentration of the ligands around each nanoparticle and the concentration of the Hg^{2+} ions. The absorption as a function of the number of Hg^{2+} equivalents necessary to stabilize the system (Figure 10). An inspection shows that for the AuNPs 2, 2 equiv of Hg^{2+} are necessary, instead of the 5 equiv for the AuNPs 1. The AuNPs 2 is more sensitive to mercury (II) than AuNPs 1 [40-43] Scheme 3.

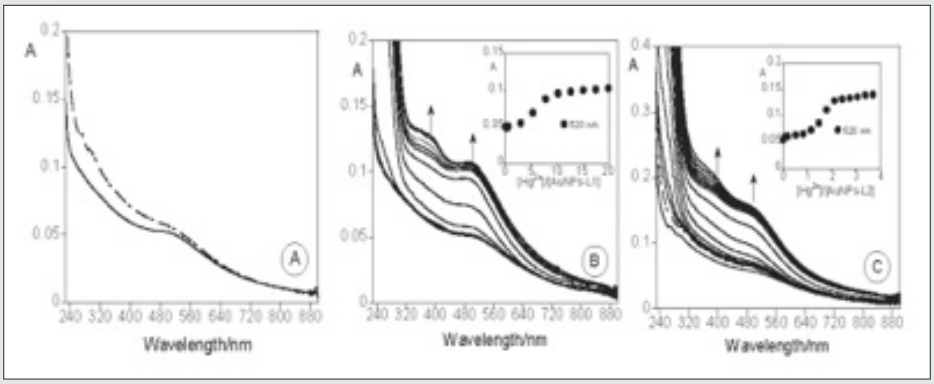

Figure 10: (A) Absorption spectrum of AuNPs with compound 1 (full line) and 2 (dotted line). Spectrophotometric titration of AuNPs with compounds 1 (B) and 2 (C) with the addition of Hg^{2+} ions in dichloromethane. ([1] = 1.24 × 10^{-5} M, [2] = 6.35 × 10^{-6} M, [Hg^{2+}] = 6.01 ×10^{-3} M, room temperature).

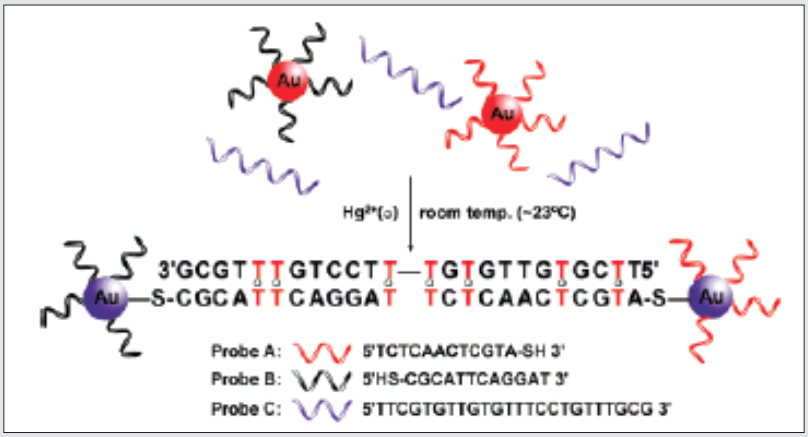

Scheme 3: basic design of our sensor system for Hg^{2}

Colorimetric Detection of Mercury (Hg^{2+}) Using DNA/Nanoparticle Conjugates

A novel and practical system for colorimetric detection of mercury at room temperature. The system utilizes a combination of oligonucleotides and NPs at low concentrations, which readily detects Hg^{2+} in aqueous solutions and in the presence of an excess of other metal ions [44]. The method can be rationalized for use to detect other metal ions by replacing natural DNA bases with metal-dependent synthetic artificial bases [45]. To achieve this goal, a fundamentally different design was taken, making use of DNA/NP conjugates and thymine-Hg^{2+}-thymine (T-Hg^{2+}-T) coordination chemistry [46] to develop a sensor system that operates within an adjustable operating temperature range and rapidly detects mercury in a single step. The basic design of our sensor system for Hg^{2+} is composed of three elements as shown in (Scheme 3). Two types of DNA-functionalized gold NP probes [47] (designated as probe A, Au-3'S-ATGCTCAACTCT5', and probe B, Au-5'S-CGCATTCAGGAT3'), and an appropriate oligonucleotide linker (designated as probe C). To choose a specific sequence for the probe C, one has to ensure that it recognizes the particle probes A and B and forms stable DNA duplexes (or NP aggregated networks) only in the presence of Hg^{2+} at a given operating temperature. In the absence of Hg^{2+}, these three probes do not form DNA/NP aggregates because of a lower melting temperature (Tm) than the operating temperature due to mismatches formed in the DNA duplexes. Importantly, by controlling the number of T-T mismatches in the system, one can precisely modulate the melting temperature of the three probes within a specific range. To this regard, it has been studied temperature profiles using UV-vis spectroscopy for a series of probe solutions containing oligonucleotide linkers (probes C1-7) that are complementary to probes A and B except for various numbers of the T-T mismatch. As anticipated, melting temperatures of the probes A, B, and C1-7 were decreased from 50.3, 48.6, 40.0, 34.2, 26.2, 22.8, to 21.3°C with an increasing number of T-T mismatches. It should be noted that the melting temperature of the probes can be further suppressed well below the operating ambient temperature (23°C) with a solution containing eight T-T mismatches (probes A*, B, C7; Tm) 14.4°C) as shown in (Figure 11).

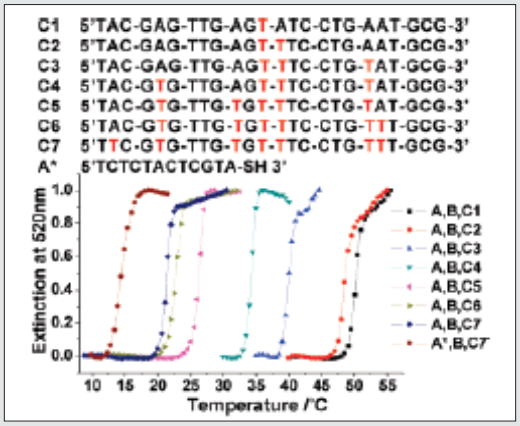

Figure 11: Normalized melting curves of solutions containing probes A (or A*), B and the linker probes $\mathbf{C}_{1\text{-}7}$ with varied numbers of T-T mismatches.

As a proof-of-concept experiment, an aqueous solution of Probes A, B, and C7 (2 nM, 2 nM, and 1 μM, respectively; Tm) 21.3°C) was selected for a prototype sensor system for Hg^{2+} at room temperature. Upon addition of an aqueous solution of Hg^{2+} (10 μM), a clear red-to-purple/pinkish colorimetric response occurred within 5 min (Figure 12a). The particle-amplified color change indicates formation of stable Hg^{2+}-mediated DNA base pairs as evidenced by an increase in the sharp melting temperature (42.4°C) shown in (Figure 12c). The UV-vis spectrum of the solution also shows a bathochromic shift of the gold nanoparticles from 520 to 565 nm, indicating the formation of particle aggregates via Hg^{2+} induced hybridization events. The NP aggregates were confirmed by transmission electron microscopy in contrast to dispersed NPs in the absence of Hg^{2+}. To exclude the possibility that Hg^{2+} may directly remove the thiolated oligonucleotides from the surface of the particles because of its thiophilic nature [48], we performed control experiments without the oligonucleotide linker (probe C7). Upon addition of various concentrations of Hg^{2+} (10, 50, and 100 μM), we did not observe visible color changes (or particle precipitation) over a period of time of 48 h (Figure 12a, Blank2). Taken together, these observations suggest that the rapid assembly of the nanoparticles at ambient temperature is indeed attributed to the formation of stable T-Hg^{2+}-T base pairs in DNA duplexes.

In a further set of experiments, selectivity of metals ions was studied. Solutions containing metal ions (Co^{2+}, Pb^{2+}, Ni^{2+}, Cu^{2+}, Ca^{2+}, Mn^{2+}, Sn^{2+}, Zn^{2+}, $Ru^{3+}$and Fe^{3+}; each at 10 μM) were tested under the same conditions as in the case of Hg2+. Remarkably, no optical and thermal transition profile changes of the solutions were observed with these metal ions up to millimolar concentrations (Figure 12a).

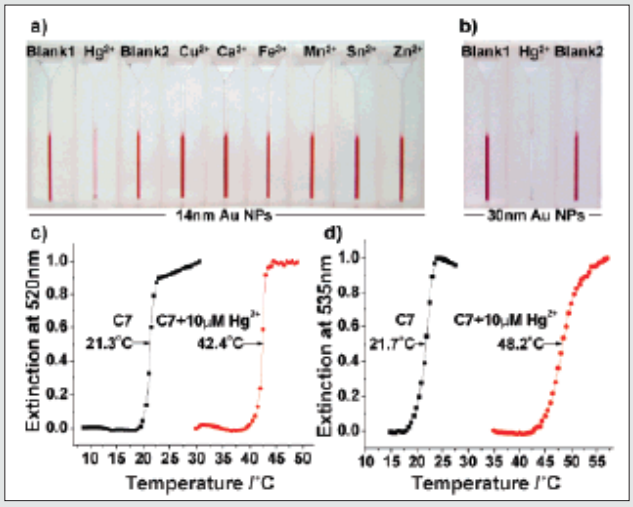

Figure 12: (a) Color response of a 14 nm NP detection system (probes A, B, and C_7) in the presence of a selection of metal ions (Hg^{2+}, Cu^{2+}, Ca^{2+}, Fe^{3+}, Mn^{2+}, Sn^{2+}, Zn^{2+}; 10 μM each). Note that **Blank1** (probes A, B, and C7 without Hg^{2+}) and **Blank2** (probes A and B with Hg^{2+}) were used as control references. (b) Color response of a 30 nm NP detection system under the same conditions. (c, d) Normalized melting curves of the solution (containing probe A, B, and C_7) with or without Hg^{2+} (10 μM) for the 14 and 30 nm NP systems, respectively.

The specific detection for Hg^{2+} is clearly attributed to its selective binding of T-T mismatches, resulting in the formation of stable T-Hg^{2+}-T complexes that lead to particle aggregation. We have also investigated the sensitivity of our detection system. Various concentrations (0.5, 1.0, 2.0, 3.0, 5.0, 10, 25, and 50 μM) of Hg^{2+} were added to a series of solutions containing 14 nm NP probes (A and B; each at 2 nM) and the oligonucleotide linker (probe C7; 1 μM). The corresponding melting temperatures were measured at 21.8, 22.3, 22.9, 24.8, 28.3, 42.4, 47.5, and 50.0 °C, respectively. The limit of detection for the 14 nm NP systems by the naked eye is about 3 μM of Hg^{2+}.However, the sensitivity of the system can be further improved (1μM) by using larger particles or varying oligonucleotide sequences on the surface of the nanoparticles.

For example, upon addition of Hg^{2+} (10 μM) to a solution containing 30 nm particles, an enhanced color change can be readily observed (Figure 12b). The signal enhancement of the 30 nm NP system was attributed to significant extinction dampening in the plasmon region of the spectrum that accompanies Hg^{2+}-induced NP aggregation. In contrast to the 14 nm NP counterpart, a larger melting transition (e.g., 27 versus 21 °C with 10 μM of Hg^{2+}) was observed for the 30 nm NP solution between the dispersed and aggregated states (Figure 12d).

Colorimetric And Fluorometric Chemosensors For Selective Signaling Toward Ca^{2+} And Mg^{2+} By Aza-Crown Ether Acridinedione-Functionalized Gold Nanoparticles

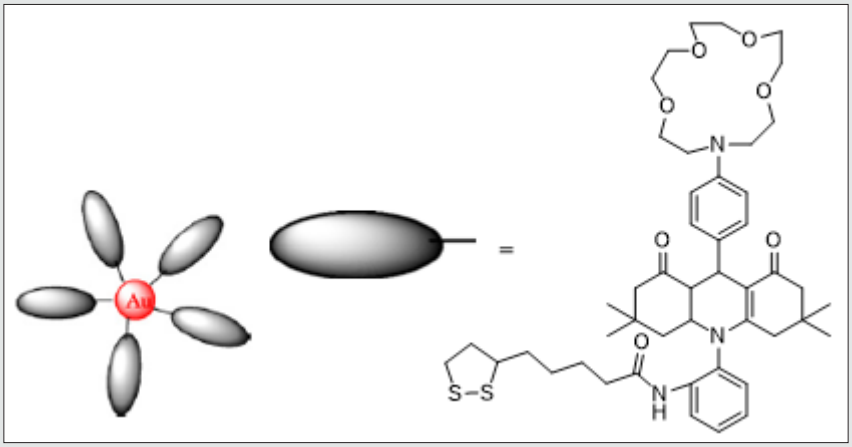

Figure 13: Structure of aza-crown ether acridinedione-functionalized gold nanoparticles (ACEADD-GNPs) 3

The aza-crown ether acridinedione-functionalized gold nanoparticles (ACEADD-GNPs) 3 have been synthesized and investigated as a fluorescent chemosensor for metal ions. A blue shift along with an intensity enhancement of emission and color change are observed in the presence of both Ca2+ and Mg2+ ions. The enhanced fluorescence intensity is attributed to the photoinduced electron transfer (PET) suppression through space and color change of the suspension from red to blue due to shifted surface plasmon resonance (SPR) with aggregation of nanoparticles by the sandwich complexation (Figure 13) [49]. Aza-crown ether acridinedione-GNPs exhibit the absorption spectrum of ACEADD-GNPs (3) that consists of two bands: (i) the additive absorption spectrum of ACEADD due to ICT around 360 nm and (ii) a broad band in the visible region around 529 nm, which is attributed to the surface plasmon resonance (SPR) for the stabilized gold nanoparticles. Crown ethers are known for the unusual property of forming stable complexes with alkali metals. The exceptional stability correlates, to some extent, with the close fit of the cation to the crown cavity where, upon complexation, the oxygen atoms lie in a nearly planar arrangement about the central cation. Although 15-crown-5 complexes best with Na+ and 18-crown-6 favors K+, a sandwich complex of 2:1 between 15-crown-5 and K+ is also well known [50–58].

Interestingly, addition of Na+ and K+ ions did not alter the absorption or emission properties of (3). In contrast, on the addition of Ca^{2+} or Mg^{2+} ions (0–9.6 × 10-5 M), the acetonitrile solution of 6 (2.5 × 10-5 M) showed a red shift in the absorption maximum. The significant change in the color visible to the naked eye demonstrates that the ACEADD-GNPs recognize Ca^{2+} and Mg^{2+} and lead to the nano aggregation (Figure 14). A highly specific, for both Ca^{2+} and Mg^{2+} ions, binding event is achieved by the cation-induced sandwich-like structure of the aza-crown ether acridinedione-GNPs Scheme-4 and the resultant nano-Au aggregation through colorimetric response that is indicated by broadening and red shifting of surface plasmon resonance peak as reported by Patel et al [59] and Lin et al [60].

The ACEADD-capped gold nanoparticle's colloidal solution appears red (Figure 15). However, upon addition of Ca^{2+} and Mg^{2+} the solution immediately turns blue. The significant change in color demonstrates that the ACEADD-GNPs recognize Ca^{2+} and Mg^{2+}. Surprisingly, a pronounced blue shift along with an intensity enhancement of the ACEADD-GNPs emission was observed for (3) in the presence of Ca^{2+} and Mg^{2+}. An intensity maximum is reached at [M2+]/4 = 2.5 × 10-5 M, and the emission maximum shifts as much as 40 nm (from 440 to 400 nm), when excited at 360 nm as shown in (Figures 15,16). The corresponding additive absorption

spectrum of ACEADD is not affected but SPR peak is shifted. The spectral features of blue shifted and intensity enhanced emission are retained, albeit to a lesser extent, and requiring a higher ratio of metal ion concentration. With lower concentration of metal ion, the emission maximum is at 420 nm. The kmax continues to shift toward blue upon further addition of Ca^{2+} or Mg^{2+} (e.g. kmax = 400 at $[M^{2+}]/4$ = 2.5 × 10-5 M). Apparently, the interactions between 3 and metal ions are weak and the ACEADD-GNPs emission indicates a symmetrical sandwich-like structure; the blue shifted form is generally attributed to partially overlapping crown ether moiety of ACEADD, which might account for the weak emission of blue shifted ACEADD-GNPs and poor sensitivity of the ACEADD emission to the ground state structure. Accordingly, the binding of Ca^{2+} or Mg^{2+} in (3) not only brings the crown group together in the ground state leading to the formation of a sandwich but also prohibits or minimizes such a relaxation event in the excited state leading to a blue shifted emission. The enhancement in fluorescence intensity is attributed to the suppression of the PET process through space.

Addition of other metal ions such as Na+, K+, Sr^{2+} and Ba^{2+} showed only marginal changes to the d emission of (3), when compared to those with both Ca^{2+} and Mg^{2+} ions.

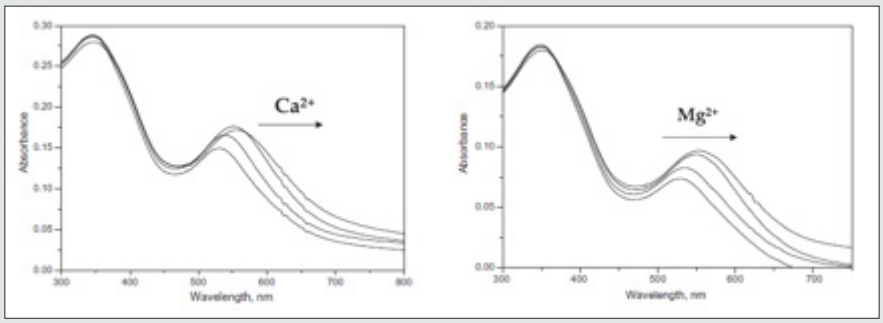

Figure 14: The absorption spectra of 6 upon addition of Ca^{2+} and Mg^{2+} in acetonitrile.

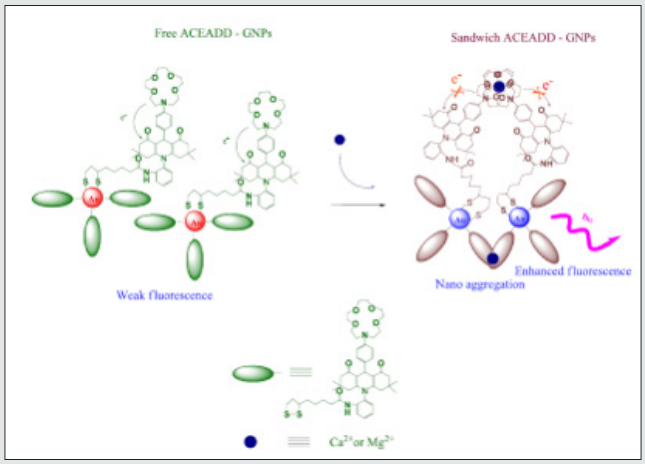

Scheme 4: The possible mechanism of the phenomenon of binding of the free ACEADD-GNPs with Ca^{2+} and Mg^{2+}.

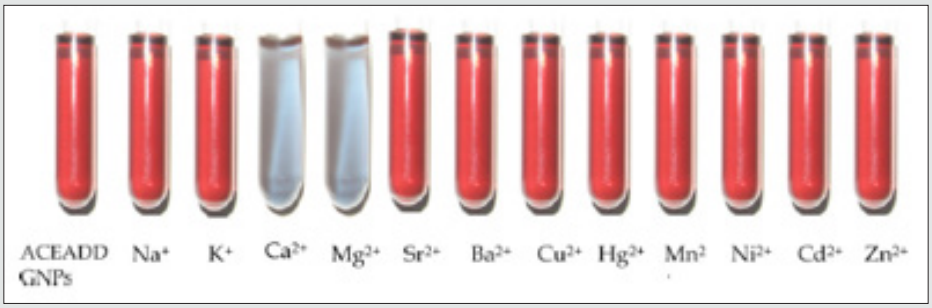

Figure 15: Colorimetric responses of ACEADD-GNPs colloidal solutions appear red. However, upon addition of Ca^{2+} (9.6 × 10^{-5} M) and Mg^{2+} (9.6 × 10^{-5} M) the solution immediately turns blue. Addition of other metal ions did not affect the color change.

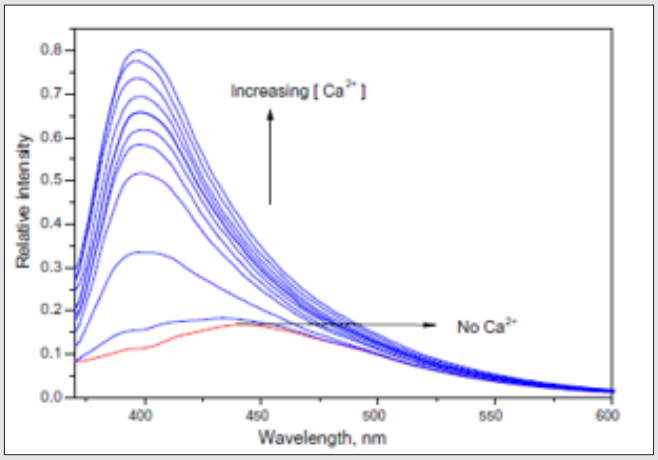

Figure 16: The emission (k_{ex} = 360 nm) spectra of **3** upon addition of Ca^{2+} (0–9.6 × 10^{-5} M) in acetonitrile.

Colorimetric Chemosensors To Metal Nanoparticles Using Two New Tyrosine Schiff-Base Ligands For Cu^{2+} Detection

Two new tyrosine Schiff-base ligands 4 and 5 bearing an indole or a thianaphthene moiety were synthesized. The sensing ability towards Ca^{2+}, Zn^{2+}, Cd^{2+}, Cu^{2+}, Ni^{2+}, Hg^{2+} and Al^{3+} metal ions was explored in absolute ethanol. Both compounds showed colorimetric properties in the presence of Cu^{2+} ions, changing their colour from light yellow to purple (4) and dark pink (5). The minimal amount of Cu^{2+} that compounds 4 and 5 could quantify was ca. of 8 ppm. In order to obtain new nanomaterials based on the reported systems, new gold and silver nanoparticles were successfully synthesized by self-reduction of compound 4 in an aqueous alkaline environment. A size distribution with a peak almost symmetrically centered on 12 ± 3.5 nm for AgNPs, and a distribution quite asymmetrical with an average size of 7.50 ± 6 nm for AuNPs were determined by TEM images. In the case of gold nanoparticles the poly disperses distribution suggested some nanoparticle aggregation [61]. The sensing ability of compounds 4 and 5 were carried out in the presence of Ca^{2+}, Zn^{2+}, Cd^{2+}, Cu^{2+}, Ni^{2+}, Hg^{2+} and Al^{3+} in absolute ethanol solutions. Compound 4 presented spectral changes only in the presence of Zn^{2+} and Cu^{2+}.(Figure 17) presents the spectral behavior of compound 5 with the addition of Zn^{2+} metal ion. The addition of Zn^{2+} induces a small decrease in the absorption band at 300 nm, and a red shift from 350 to 378 nm, with an isosbestic point at 369 nm. The appearances of an isosbestic point at 369 nm means that there are two different species in equilibrium. The complexation constant observed was logK1-1 = 5.110 ± 0.002, suggesting the formation of the mononuclear complex. Based on Pearson's rule and the spectral modifications, the interaction of the metal ion probably occurs between the nitrogen donors atoms presented in the molecule [62]. Compound 5 shows similar results with Zn^{2+} and Cd^{2+}, which can be seen in (Figure 18 A), which shows the spectrophotometric titration in the presence of Zn^{2+}. On a careful inspection of (Figure 18 A), with the increase of Zn^{2+} ions, a decrease in the absorption at 300 nm is observed, followed by the appearance of band at 350 nm with an isosbestic point at 330 nm.

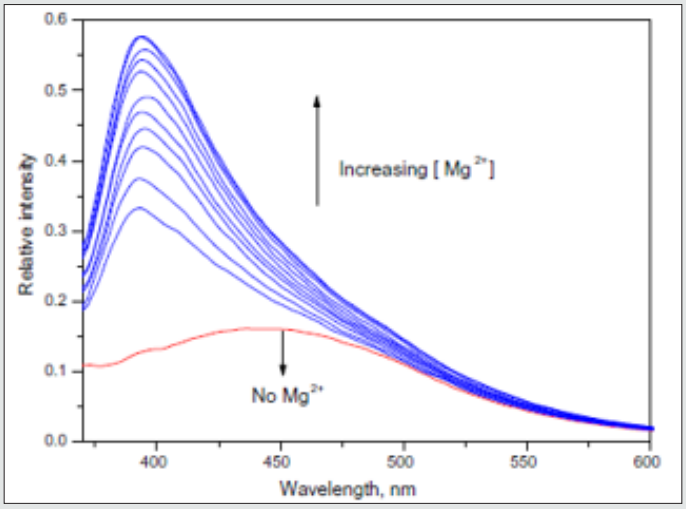

Figure 17: The emission (k_{ex} = 360 nm) spectra of **3** upon addition of Mg^{2+} (0–9.6 × 10^{-5} M) in acetonitrile.

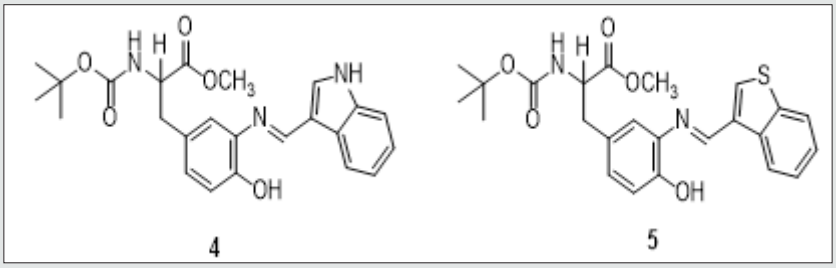

Figure 18: Structure of tyrosine Schiff-base ligands 4 and 5

Similar results were observed for compound 4. The complexation constant for both metal ions, Zn^{2+} and Cd^{2+} was very similar, logK1-1 = 5.256 ± 0.002 for Zn^{2+} and logK1-1 = 5.253 ± 0.002 for Cd^{2+}, which suggests that the complex formation involves the same donor atoms. The addition of Ca^{2+} to compound 5 (Figure 19 B) only produces a small quenching in the absorption at 300 nm, without the band formation at 350 nm. The formation constant has a stoichiometry metal: ligand 1:2, log K = 11.29 ± 0.01, leading us to the formation of a different complex, involving two ligands. This result suggest that compound 5 forms more stable metal complexes with Ca^{2+} than with Zn^{2+} and Cd^{2+}. Due to the presence of a sulphur atom, we also explore compound 5 for mercury (II) ions (see Figure 20). Addition of increased amounts of metal-salt in absolute ethanol induces to a red shift in the absorption band of 16 nm, and the appearance of a new band at 375 nm, corresponding to the complex stoichiometry metal: ligand 1:1, with a formation constant, of logK1-1 = 2.978 ± 0.01. According, to Pearson's law [62] the interaction within the metal ions probably involves the sulphur donor atom. A colorimetric chemosensor can be described by 4 and 5 in the presence of copper (II) ions [63, 64]. Electronic transitions, such as, charge transfer and d–d transitions might occur in compounds with transition metal ions developing optical ways for sensing. Thus, if a charge transfer transition occurs, an electron of a ligand orbital interacts with another orbital centered in the metal, giving rise to a ligand–metal charge transfer (LMCT) transition, resulting in a coloured complex [65].

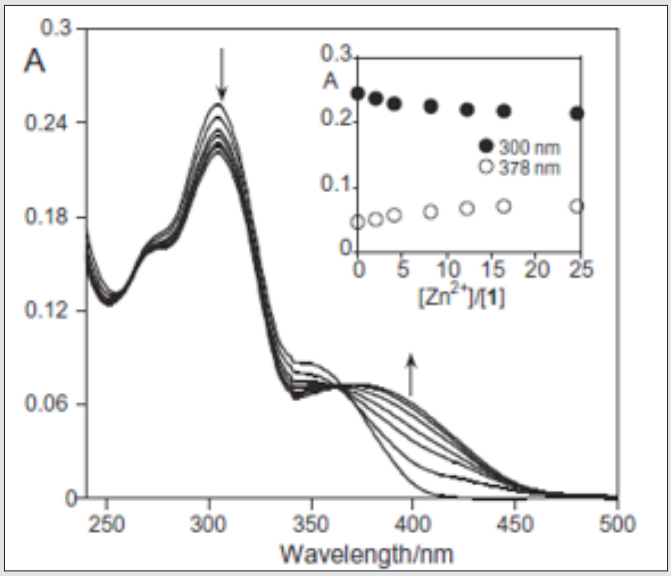

Figure 19: Spectrophotometric titration of compound 4 with the addition of Zn2+ in absolute ethanol ([4] = 1.14 × 10-5 M, T = 298 K).

The complexation constants in both cases were calculated using HypSpec [66] obtaining a logK1-1 = 3.06 ± 0.01 for compound 4 and a logK1-1 = 4.269 ± 0.001 for 5. In comparison, compound 5 shows the strongest value for Cu (II). Based on the tyrosine properties, which are easily oxidizing [67], and on the unfiled d orbital of Cu^{2+}, a LMCT band is formed for 4 at 530 nm and for 5 at 510 nm. Due to the change of colour and in metal complexes of tyrosine reported on literature, the copper (II) metal ion coordination could involve the oxygen and nitrogen donor atoms of tyrosine [68]. The detection (LOD) and quantification (LOQ) limits were determined in absolute ethanol. For compound 4 the values at 530 nm were of 0.006 ± 0.001 (LOD) and of 0.010 ± 0.001 (LOQ); and for compound 5 the values at 510 nm, were of 0.005 ± 0.001 (LOD) and of 0.009 ± 0.001 (LOQ). Taking into account these results, the minimal amount of

Cu^{2+} that might be sensed in absolute ethanol is ca. 8 ppm. Several in situ copper (II) titrations were performed using compound 4 by MALDI-TOF-MS without any other external organic matrix, using the layer by layer technique [69], where a drop of metal ion containing one equivalent was added over the dried ligand spotted on the MALDI-TOF-MS plate (1 µg/ml). The interaction between compound 4 and Cu^{2+} shows peaks corresponded to the complex species $[(4)\ Cu(BF_4)_2]^+$ at 676.5 (676.0) and $[(4)\ 2(Cu(BF_4)_2).CH_3CN]^+$ at 954.5 (954.0), which confirms the Complexation of 5 by the one and two Cu^{2+} metal ions in the gas phase. The formation of AuNPs was indicated by the appearance of dark red color and of the gold plasmonic band at 520 nm; and the AuNPs by the appearance of a yellow colour and a surface Plasmon resonance at 415 nm (Figure 21,22). Moreover, several studies of absorption and emission spectroscopy were performed, with the aim to confirm the anchoring of the compound 4 to the metal nanoparticle surface. The resulting nanoparticles were extracted three times with dichloromethane to remove the unlinked products.

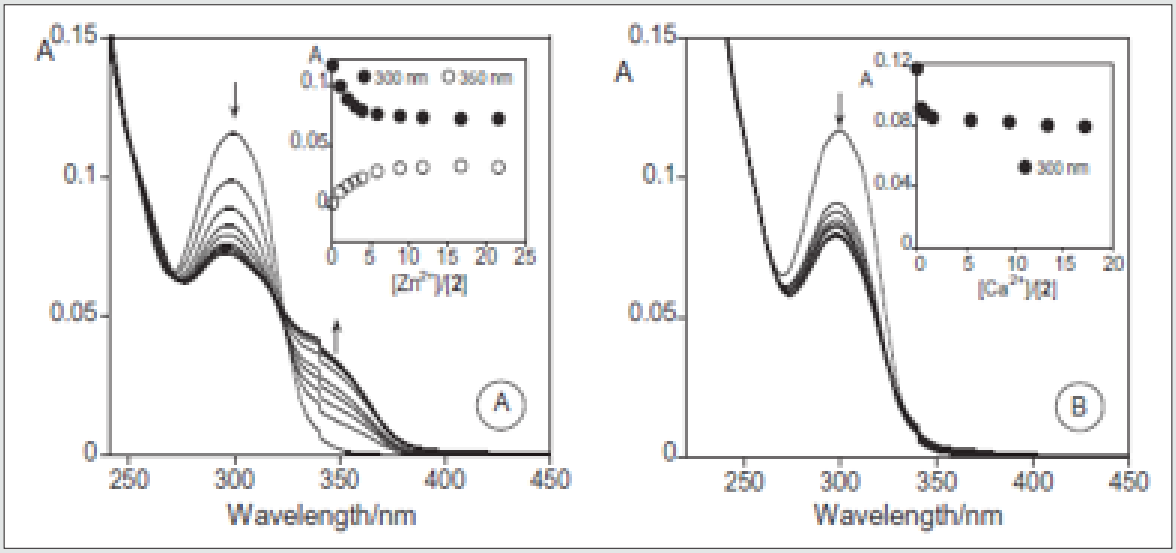

Figure 20: Spectrophotometric titration of compound 5 (A and B) with the addition of Zn2+ (A) and Ca2+ (B) in absolute ethanol ([5] = 9.53 × 10-6 M, T = 298 K).

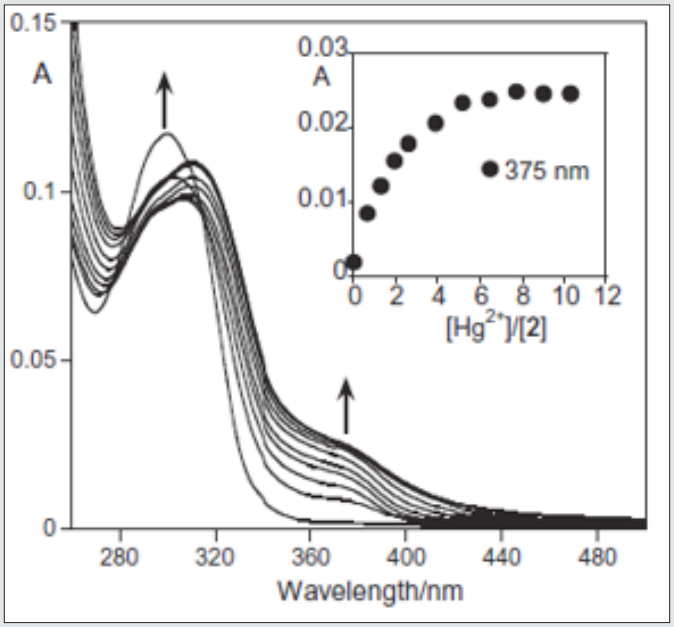

Figure 21: Spectrophotometric titration of compound 5 with the increased addition of Hg2+ in absolute ethanol. The inset shows the absorption as function of [Hg2+]/ [2] at 375 nm ([5] = 9.53 × 10-6 M, [Hg2+] = 9.22 × 10-3 M, T = 298 K).

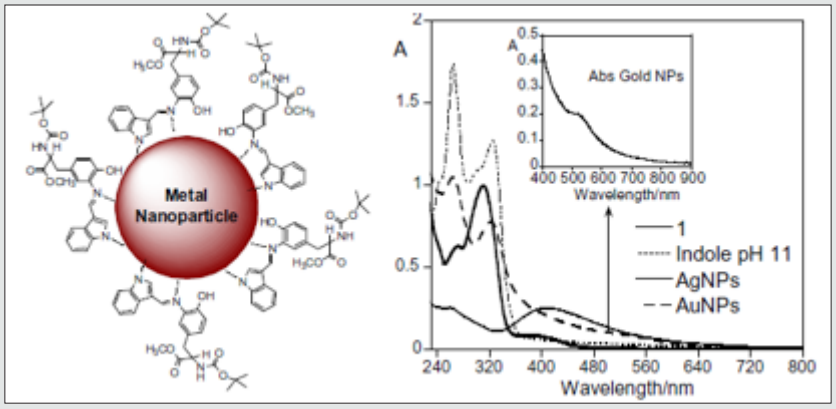

Figure 22: (Below, left) Schematic structure of the MNPs with compound 4. (Below, right) Absorption spectra of MNPs (aqueous phase), in water, T = 298 K.

References

1. Bănică, Florinel-Gabriel (2012) Chemical Sensors and Biosensors: Fundamentals and Applications. Chichester, John Wiley & Sons, UK, 576.
2. Takagi M (1990) "Cation Binding by Macrocycles," Eds. Inoue Y, Gokel GW, Dekker. New York 465.
3. Kaneda T, Umeda S, Tanigawa H, Misumi S, Kai Y, et al. (1985) Am Chem Soc 107: 4802.
4. Kubo Y, Maruyama S, Ohhara N, Nakamura M, Tokita SJ (1727) Chem. Soc Chem. Commun 1727.
5. Oueslati F, Dumazet-Bonnamour I, Lamartine R (2003) New J Chem 27: 644.
6. Gale PA, Coord Chem Rev (2003) 240: 191. (b) Gale, P. A. Coord. Chem. Rev (2001) 213: 79.
7. Suksai C, Tuntulani T (2003) Chem Soc. Rev 32: 192.
8. Cabell LA, Best MD, Lavigne JJ, Monahan MK, Anslyn EVJ (2001) Chem Soc Perkin Trans 2: 315.
9. Shihadeh YA, Benito A, Lloris JM, Martínez-Máñez R (2005) Inorg. Chem. Commun 3: 563.
10. Gale PA, Hursthouse MB, Light ME, Sessler JL, Warriner CN, Zimmerman RS (2001) Tetrahedron Lett 42: 6759.
11. Dos Santos CMG, Harte AJ, Quinn SJ, Gunnlaugsson T (2008) Coord. Chem. Rev 252: 2512.
12. Wong KMC, Yam VWW (2007) Coord. Chem. Rev 251: 2477.
13. Beer PD, Bayly SR (2005) Top1. Curr. Chem 255: 125.
14. Beer PD, Hayes, EJ (2003) Coord. Chem. Rev 240: 167.
15. Sun SS, Lees AJ (2002) Coord. Chem. Rev. 230: 171.
16. Bondy CR, Loeb SJ (2003) Coord. Chem. Rev 240: 77.
17. Sessler JL, Camiolo S, Gale PA (2003) Coord. Chem. Rev. 240: 17.
18. Bucher C, Zimmerman RS, Lynch V Sessler JL (2001) J. Am. Chem. Soc 123: 9716.
19. Amendola V, Esteban-Gomez D, Fabbrizzi L, Licchelli M (2006) Acc. Chem. Res 39: 343.
20. Gunnlaugsson T, Davis AP, Glynn M (2001) Chem. Commun 2556.
21. Lee DH, Lee KH, Hong JI (2001) Org. Lett 3: 5.
22. Cho E J, Moon JW, Ko SW, Kim SK, Yoon J, Nam KC J (2003) Am. Chem. Soc125: 12376.
23. Starnes SD, Arungundram S, Saunders CH (2002) Tetrahedron Lett 43: 7785.
24. Gerasimchuk OA, Mason S, Llinares JM, Song MP, Alcock NW, et al. (2000) Inorg. Chem 39: 1371.
25. Camiolo S, Gale PA, Light ME, Hursthouse MB Supramol (2001) Chem 13: 613.
26. Gunnlaugsson T, Glynn M, Tocci nee Hussey GM, Kruger PE, Pfeffer FM (2006) Coord. Chem Rev 250: 3094.
27. Houk RJT, Tobey SL, Enslyn EV (2005) Top. Curr. Chem 255: 199.
28. Lhotak P (2005) Top. Curr. Chem 255: 65.
29. Boiocchi M, Boca LD, Gómez DE, Fabbrizzi L, Licchelli M, et al. (2004) J. Am. Chem. Soc 126: 16507.
30. Gómez DE, Fabbrizzi L, Licchelli M, Monzani E (2005) Org. Biomol. Chem. 3: 1495.
31. Gunnlaugsson T, Kruger PE, Lee TC, Parkesh R, Pfeffer FM, et al. (2003) Tetrahedron Lett 44: 6575.
32. Guomei Z, Yinghui L, Jie X, Caihong Z, Shaomin S, et al. (2013) Glutathione-protected fluorescent gold nanoclusters for sensitive and selective detection of Cu2+, Sensors and Actuators B 183: 583-588.
33. Muhammed MA, Verma P, Pal S, Retnakumari A, Koyakutty, M, et al. (2010) Luminescent quantum clusters of gold in bulk by albumin-induced core etching of nanoparticles: metal ion sensing, metal-enhanced luminescence and biolabeling, Chemistry. A European Journal 16: 10103-10112.
34. Elisabete O, Cristina N, Benito RG, Jose LC, Carlos L (2011) Novel Small Stable Gold Nanoparticles Bearing Fluorescent CysteineCoumarin Probes as New Metal-Modulated Chemosensors, Inorg. Chem 50: 8797–8807.
35. Grazul, M, Budzisz (2009) E. Coord. Chem. Rev 253: 2588.
36. Gans P, Sabatini A, Vacca A (1996) Talanta 43: 1739.
37. Santos HM, Pedras B, Tamayo A, Casabo J, Escriche, L, et al (2009) Inorg. Chem. Commun 12: 1128.

38. Sheldrick GM (1997) SHELXS97, A Computer Program for the Solution of Crystal Structures from X-ray Data; University of G€ottingen: G€ottingen, Germany.

39. Pearson RGJ (1963) Am. Chem. Soc 85: 3533.

40. Ke L, Yi Z, Cheng Y (2011) A highly sensitive and selective ratiometric and colorimetric sensor for Hg2+ based on a rhodamine–nitrobenzoxadiazole conjugate, Inorganic Chemistry Communications 14: 1798-1801.

41. Zhou Y, Zhu CY, Gao XS, You XY, Yao C (2010) Organic Letters 11: 2566-2569.

42. Shi W, Ma HM (2008) Chemical Communications 16: 1856-1858.

43. Liu W, Xu LW, Zhang HY, You JJ, Zhang XL, et al. (2009) Organic and Biomolecular Chemistry 7: 660-664.

44. Xue X, Wang F, Liu X (2008) One-Step, Room Temperature, Colorimetric Detection of Mercury (Hg2+) Using DNA/Nanoparticle Conjugates, J. AM. CHEM. SOC 130: 3244-3245.

45. Ogawa AK, Wt Y, Berger M, Schultz PG, Romesberg FEJ (2000) Am. Chem. Soc 122: 8803.

46. Katz SJ (1952) Am. Chem. Soc. 74: 2238.

47. Mirkin CA, Letsinger RL, Mucic RC, Storhoff JJ (1996) Nature 382: 607.

48. Cotton FA, Wilkinson G, Murillo CA, Bochmann M (1999) Advanced Inorganic Chemistry; Wiley: New York.

49. Velu R, Ramakrishnan VT, Ramamurthy P (2010) Colorimetric and fluorometric chemosensors for selective signaling toward Ca^{2+} and Mg^{2+} by aza-crown ether acridinedione-functionalized gold nanoparticles, Tetrahedron Letters 51: 4331-4335.

50. Xiong D, Li H (2008) Nanotechnology 19: 465502.

51. Masilamani D, Lucas ME (1992) In Fluorescent Chemosensors for Ion and Molecule Recognition; Czarnik, A. W, Ed, American Chemical Society: DC Washington.

52. Inoue Y, Gokel GW (1990) Cation Binding by Macrocycles: Complexation of Cationic Species by Crown Ethers; Dekker: New York.

53. Bradshaw JS, Krakowiak KE, Izatt RM (1993) Aza-Crown Macrocycles; John Wiley and Sons: New York.

54. Toupance T, Benoit H, Sarazin D, Simon JJ (1997) Am. Chem. Soc 119: 9191.

55. Boldea A, Levesque I, Leclerc MJ (1999) Mater. Chem 9: 2133.

56. Flink S, Boukamp BA, van den Berg A, van Veggel FCJM, Reinhoudt DNJ (1998) Am. Chem. Soc. 120: 4652.

57. Flink S, van Veggel FCJM, Reinhoudt DNJ (1999) Phys Chem B 103: 6515.

58. Kimura K, Harino H, Hayata E, Shono T (1986) Anal. Chem 58: 2233.

59. Patel G, Kumar A, Pal U, Menon S (2009) Chem. Commun 1849.

60. Yi Lin, S, Wei Liu, S, Mei Lin, C, Chen CC (2002) Anal. Chem 74: 330.

61. Elisabete O, Júlio DN, Hugo MS (2012) From colorimetric chemosensors to metal nanoparticles using two new tyrosine Schiff-base ligands for Cu^{2+} detection. Inorganic Chimica Acta 380: 22-30.

62. Pearson RGJ (1962) Am. Soc 84: 62.

63. Lodeiro C, Capelo JL, Santos HM, Pedras B, Nuñez C (2010) Chem. Soc. Rev 39: 1.

64. Bernard V (2001) Molecular Fluorescence: Principles and Applications, Wiley-VCH Verlag GmbH.

65. Dunn TM, Lewis J, Wilkins RG (1960) Modern Coordination Chemistry, New York: Interscience. Chapter 4, Section 4, "Charge Transfer Spectra 268.

66. Gans P, Sabatini A, Vacca A (1996) Talanta 43: 1739.

67. Si S, Bhattacharjee RR, Banerjee A, Mandal TK (2006) Chem. Eur. J. 12: 1256.

68. Sipos P, Kiss TJ (1990) Chem. Soc, Dalton Trans 2909.

69. Fernández-Lodeiro J, Nuñez,C, Carreira R, Santos HM, Capelo JL, Lodeiro C (2011) Tetrahedron 67 : 326 RG Pearson J (1962) Am Soc 84: (16):62.

DOI: 10.32474/MAMS.2021.04.000200